Science Translational Medicine
AAAS

stm.sciencemag.org/cgi/content/full/11/492/eaav4508/DC1

Supplementary Materials for

Cediranib suppresses homology-directed DNA repair through down-regulation of BRCA1/2 and RAD51

Alanna R. Kaplan, Susan E. Gueble, Yanfeng Liu, Sebastian Oeck, Hoon Kim, Zhong Yun, Peter M. Glazer*

*Corresponding author. Email: peter.glazer@yale.edu

Published 15 May 2019, *Sci. Transl. Med.* **11**, eaav4508 (2019)
DOI: 10.1126/scitranslmed.aav4508

The PDF file includes:

Materials and Methods
Fig. S1. Cediranib suppresses expression of HDR factors in cancer cells in culture.
Fig. S2. Effects of cediranib on HDR factor expression are not mediated through a trans-acting factor.
Fig. S3. Inhibition of VEGFRs does not suppress HDR factor expression.
Fig. S4. Inhibition of PDGFRs suppresses HDR factor expression.
Fig. S5. siRNA-mediated targeting of *PDGFR*β suppresses HDR factor expression.
Fig. S6. No consistent changes were observed in cell cycle profiles after various kinase inhibitor and siRNA treatments.
Fig. S7. Cediranib suppresses expression of FANCD2 in cancer cells in culture.
Fig. S8. PDGFR inhibition shifts migration of p130.
Table S1. Reported mutations in DNA repair genes.

Other Supplementary Material for this manuscript includes the following:

(available at stm.sciencemag.org/cgi/content/full/11/492/eaav4508/DC1)

Data file S1 (Microsoft Excel format). Individual data points.

Supplementary Materials:

Materials and Methods

Cell culture: SKOV3, MCF7, and MDA-MB-231 cells were obtained from ATCC. IGROV1 and PEO14 cells were provided by Dr. Elena Ratner (Yale University School of Medicine). PEO1 and PEO4 cells were obtained from Dr. Toshiyasu Taniguchi (Fred Hutchinson Cancer Research Center). MDA231-5XHRE-GFP cells were provided by Dr. Zhong Yun (Yale University School of Medicine). RKO-Neo and RKO-E7 cells were provided by Dr. Kathleen Cho (University of Michigan). U2OS EJ-DR and MCF7 DR-GFP cells were provided by Dr. Ranjit Bindra (Yale University School of Medicine). Cells were grown in McCoy's (SKOV3), RPMI (IGROV1, MDA-MB-231, MDA231-5XHRE-GFP, PEO1, PEO4, and PEO14), or DMEM (MCF7, U2OS EJDR and MCF7 DR-GFP) medium containing 10% fetal bovine serum without antibiotics. RKO-Neo and -E7 cells were grown in MEM medium containing 10% fetal bovine serum and 500 µg/ml G418.

Conditioned medium: SKOV3 cells were seeded at a density of $2x10^5$ cells per 10 cm dish, then treated with DMSO or cediranib for 2 hours followed by several PBS washes and replacement of medium. 24 hours later, conditioned medium from DMSO- and cediranib-treated cells was collected and centrifuged for 5 minutes at 4300 rpm. New SKOV3 cells seeded at a density of $1x10^6$ cells per 10 cm dish were treated with conditioned medium for 24 hours, then collected and processed for Western blot analysis as described above.

DNA repair luciferase reporter plasmids: To assess HDR, we used a modified gWIZ.Luciferase vector (Gelantis) containing an inactivating I-SceI recognition site in the Firefly luciferase gene with a downstream promoter-less copy of the gene that can serve as a donor template for HDR. A double strand break was introduced into this plasmid via restriction enzyme digest using I-SceI (New England Biosystems). To assess NHEJ, we used the Firefly luciferase plasmid pGL3 (Promega) and introduced a double strand break between the promoter and the luciferase gene via HindIII restriction enzyme digestion (New England Biosystems). Unmodified gWiz.Luciferase and undigested pGL3 plasmids were used as normalization controls for HDR and NHEJ, respectively. Cells were pretreated with cediranib for 6 hours before transfection of 1 µg/ml luciferase plasmids using Turbofect (ThermoFisher). 50 ng/ml of a Renilla luciferase plasmid (pCMV-RL, Promega) was transfected simultaneously as an internal transfection control. Cells were collected 24 hours after transfection, and luciferase activity was quantified using Dual Luciferase Reporter Assay (Promega). Percent reactivation was calculated by dividing Firefly luciferase activity by Renilla luciferase activity and normalizing to the control samples.

Plasmid-mediated overexpression: Plasmids containing the open reading frames for the human *PDGFRβ* and *VEGFR2* genes with C-terminal FLAG (DYKDDDDK) tags under control of the CMV promoter were obtained from GenScript (PDGFRβ: OHu25829, VEGFR2: OHu27183). SKOV3 cells were transfected with 1 µg/ml plasmids using Turbofect (ThermoFisher), and 48 hours later were treated for Western blot or cell viability analysis as described above.

Cell cycle analysis: SKOV3 cells were seeded at a density of 100,000 cells per well in a 96-well plate then treated with inhibitors for 24 hours or siRNAs for 96 hours. Cells were then fixed in

70% EtOH for 4 hours and stained with Hoescht33342 at a concentration of 1 µg/mL overnight, and washed three times with PBS. Nuclear DNA content was then analyzed on the basis of dye intensity using automated digital microscopy with a BioTek Cytation 3 Cell Imaging Multi-Mode Reader (ThermoFisher).

Kinase inhibitor screen: The kinase inhibitor screen was performed in U2OS EJ-DR cells using compounds from a commercially available kinase inhibitor library (SelleckChem) at a concentration of 10 µmol/L. DSBs were induced by the addition of triamcinolone (0.5 µM, Sigma) and Shield1 (100 nM, Clontech) to cell culture medium for 24 hours to activate the endogenously expressed I-Sce I enzyme. Cells were analyzed by flow cytometry to quantify GFP+ cells 72 hours after DSB induction. Ouabain was used as a positive control (*37*). In parallel, compound toxicity was determined using CellTiterGlo (Promega), and any compounds inducing more than 50% cytotoxicity were excluded from further analysis. Data are presented as % vehicle-treated control.

RAD51 foci: Cells were seeded in 8-chamber slides and irradiated at the next day with 2 Gy using an X-RAD 320 X-Ray Biological Irradiator (Precision X-Ray Inc). Non-irradiated controls were handled in parallel but kept outside of the irradiator during treatment. After the desired repair times, cells were fixed and permeabilized in 3% PFA/0.5% Triton-X100/2% sucrose for 20 minutes. Blocking was performed with 5% fetal bovine serum and 5% normal goat serum in PBS overnight at 4 C. Subsequently, samples were incubated with primary antibodies (anti-γ-H2A.X antibody mouse, 1:400, 05-636, EMD Millipore, and anti-RAD51 rabbit, 1:300, PC130, CalBiochem) in blocking solution overnight at 4 C. After washing with 0.5% Triton-X100 in PBS, samples were incubated with secondary antibodies [anti-mouse AF Plus 488, anti-rabbit AF Plus 555 (1:400; A32732, Thermo Fisher)] in blocking solution for 90 min at room temperature (RT). DNA was stained with DAPI (2.5 µg/mL; #1816957; Thermo Fisher) for 15 min at RT. After washes, chambers were removed from the slides and the slides were covered with coverslips using DAKO Fluorescence Mounting Medium (S3023; Dako NA Inc.) and sealed with nail polish. Images were analysed with a Nikon Eclipse Ti fluorescence microscope with a Plan Apo 60X/1.40 Oil DIC h objective, a CSU-W1 confocal scanning unit with an iXon Ultra camera (Andor Technology), MLC 400B laser unit (Agilent Technologies), and NIS Elements 4.30 software (Nikon Corporation). Foci were analysed with the Focinator v2-30 software as previously described (*39*). Representative images were generated with ImageJ.

Antibodies: The following antibodies were used for Western blotting: BRCA2 (Calbiochem, OP95), BRCA1 (Santa Cruz, sc-6954), RAD51 (Novus, NB100-148), DNA-PKcs (CST, #4602), Ku80 (BD, #611360), XLF (CST, #2854), vinculin (Abcam, ab129002), GAPDH (Santa Cruz, sc-365062), FLAG (Sigma, F7425), VEGFR2 (CST, #3479), caspase-3 (CST, #9664), cleaved PARP (CST, #9541), pPP2A(Y307) (ThermoFisher, PA5-36874), and PP2A (CST, #2259).

Quantitative real-time PCR analysis: The following premixed primers and probes were used: *BRCA2*, *BRCA1*, *RAD51*, *PRKDC*, *XRCC5*, *XRCC4*, *NHEJ1*, *PDGFRα*, *PDGFRβ*, *ACTB*, and *18S* (Applied Biosystems).

Chromatin immunoprecipitation (ChIP) primers:
Quantitative analysis was performed with RT-PCR using the following primers:

BRCA1-F: 5'-GATTGGGACCTCTTCTTACG-3'

BRCA1-R: 5’-TACCCAGAGCAGAGGGTGAA-3’
BRCA2-F: 5’-AAGCGTGAGGGGACAGATT-3’
BRCA2-R: 5’-GCCGGAGTAAGCTGACAAA-3’
RAD51-F: 5’-CCCCCGGCATAAAGTTTGAAT-3’
RAD51-R: 5’-GAAGCGCCGCACTCTCCTTA-3’

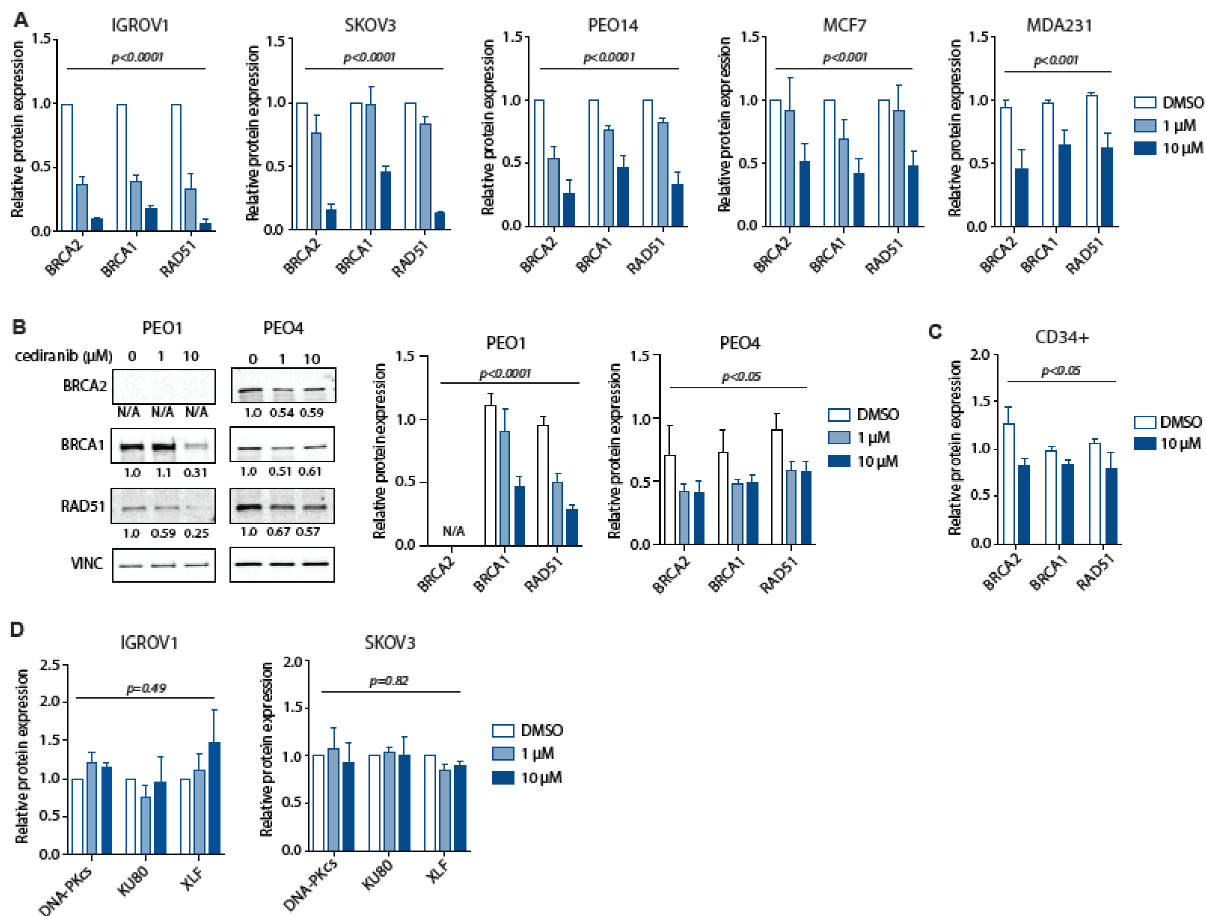

Fig. S1. Cediranib suppresses expression of HDR factors in cancer cells in culture.
(A) Quantification of Western blots of HDR factors in ovarian (IGROV1, SKOV3, and PEO14) and breast (MCF7 and MDA231) cancer cell lines treated with increasing doses of cediranib in culture (2-way ANOVA, effect of cediranib IGROV1 $p<0.0001$, SKOV3 $p<0.0001$, PEO14 $p<0.0001$, MCF7 $p<0.001$, MDA231 $p<0.001$, n=3 independent experiments). (B) Western blot of HDR factors in PEO1 (BRCA2-deficient) and PEO4 (BRCA2-proficient) ovarian cancer cell lines treated with increasing doses of cediranib in culture (2-way ANOVA, effect of cediranib PEO1 $p<0.0001$, PEO4 $p<0.05$, n=3 independent experiments). (C) Quantification of Western blots of HDR factors in primary human CD34+ hematopoietic stem/progenitor cells treated with cediranib in culture compared to control (2-way ANOVA, effect of cediranib $p<0.05$, n=3 technical replicates). (D) Quantification of Western blots of NHEJ factors in ovarian cancer cell lines treated with increasing doses of cediranib in culture (2-way ANOVA, effect of cediranib IGROV1 $p=0.49$, SKOV3 $p=0.82$, n=3 independent experiments). Data are represented as means ± SEM. Numbers below Western blot panels represent relative quantification of the respective bands normalized to loading control by densitometry.

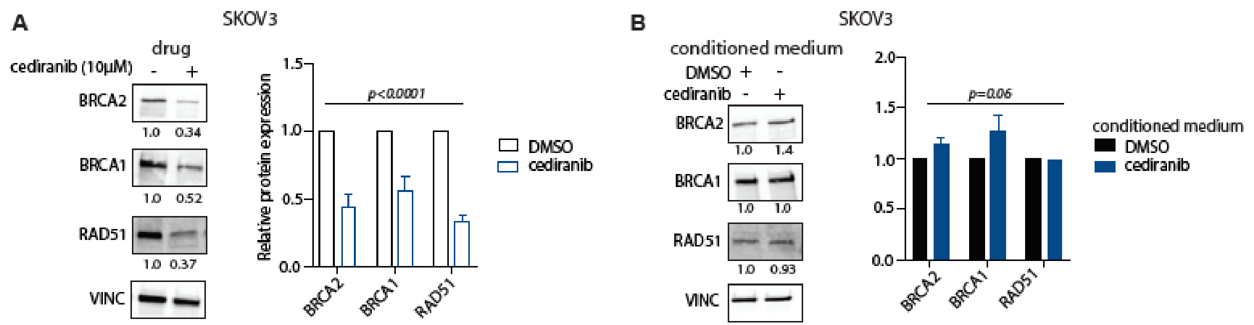

Fig. S2. Effects of cediranib on HDR factor expression are not mediated through a trans-acting factor.
Western blot of HDR factors in SKOV3 cells treated with DMSO or cediranib (A) or conditioned medium from DMSO-treated or from cediranib-treated cells (B) in culture (2-way ANOVA, effect of cediranib $p<0.0001$, effect of conditioned medium $p=0.06$, $n=3$ technical replicates). Data are represented as means ± SEM. Numbers below Western blot panels represent relative quantification of the respective bands normalized to loading control by densitometry.

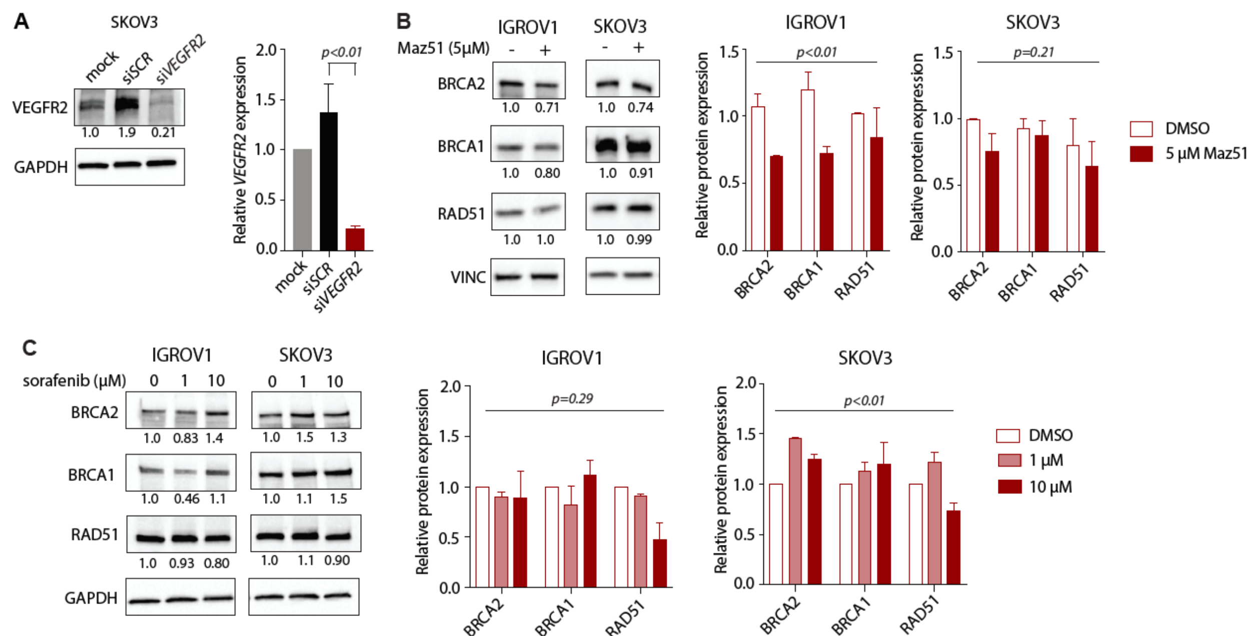

Fig. S3. Inhibition of VEGFRs does not suppress HDR factor expression.
(A) Western blot of VEGFR2 in SKOV3 cells 72 hours after treatment with *VEGFR2* siRNA (1-way ANOVA, p<0.01, si*SCR* vs. si*VEGFR2* p<0.01, n=3 independent experiments). (B) Western blot of HDR factors in IGROV1 and SKOV3 cells treated with the VEGFR3 inhibitor, Maz51, in culture (2-way ANOVA, effect of Maz51: IGROV1 p<0.01, SKOV3 p=0.21, n=3 biological replicates). (C) Western blot of HDR factors in IGROV1 and SKOV3 cells treated with the VEGFR inhibitor, sorafenib, in culture (2-way ANOVA, effect of sorafenib: IGROV1 p=0.29, SKOV3 p<0.01, n=3 biological replicates). Data are represented as means ± SEM. Numbers below Western blot panels represent relative quantification of the respective bands normalized to loading control by densitometry.

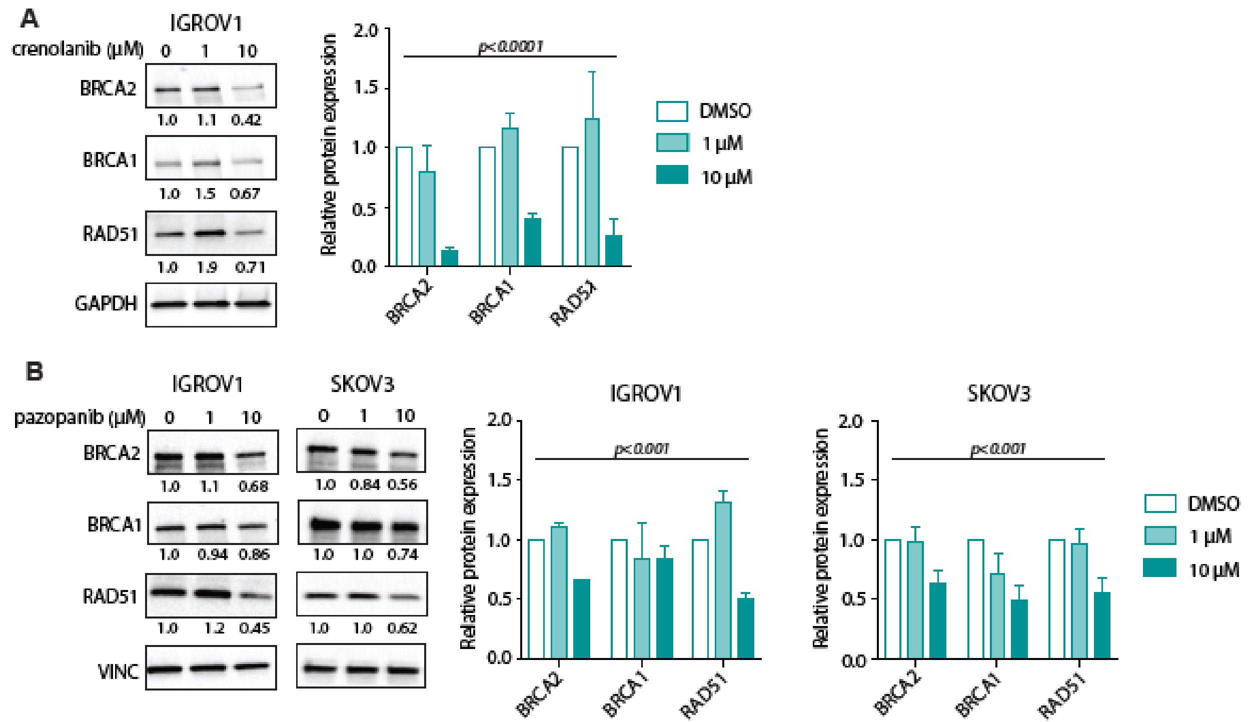

Fig. S4. Inhibition of PDGFRs suppresses HDR factor expression.
(A) Western blot of HDR factors in IGROV1 cells treated with increasing doses of the PDGFR inhibitor, crenolanib (2-way ANOVA, effect of crenolanib $p<0.0001$, n=3 independent experiments). (B) Western blot of HDR factors in IGROV1 and SKOV3 cells treated with increasing doses of the PDGFR inhibitor, pazopanib (2-way ANOVA, effect of pazopanib: IGROV1 $p<0.001$, SKOV3 $p<0.001$, n=3 independent experiments). Data are represented as means ± SEM. Numbers below Western blot panels represent relative quantification of the respective bands normalized to loading control by densitometry.

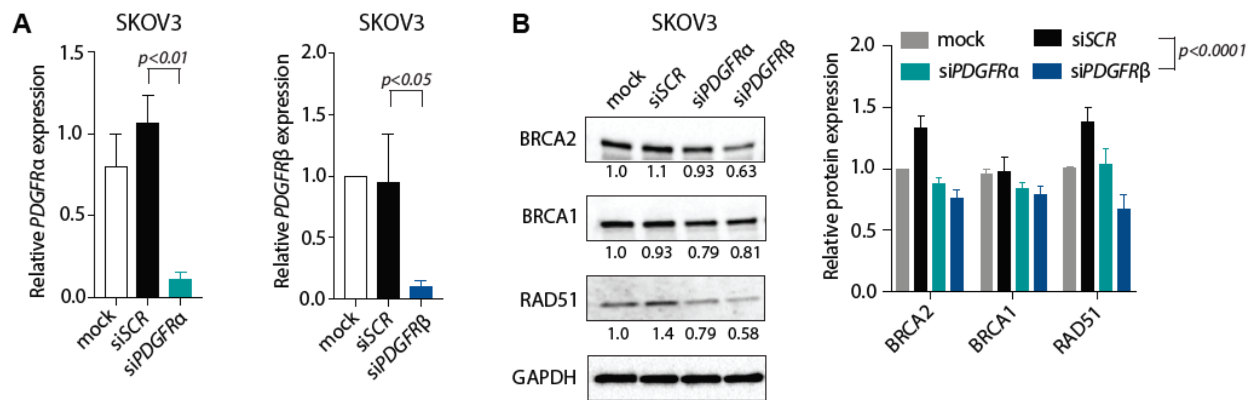

Fig. S5. siRNA-mediated targeting of *PDGFR*β suppresses HDR factor expression.
(A) Relative gene expression of *PDGFRα* and *PDGFRβ* assayed by qRT-PCR in SKOV3 cells 72 hours after treatment with *PDGFRα* and *PDGFRβ* siRNAs (1-way ANOVA, *PDGFRα* $p<0.05$; si*SCR* vs. si*PDGFRα* $p<0.01$; *PDGFRβ:* $p=0.05$; siSCR vs. *siPDGFR*β $p<0.05$, n=3 biological replicates). (B) Western blot of HDR factors in SKOV3 cells after siRNA-mediated knockdown of *PDGFRα* and *PDGFRβ* (2-way ANOVA, effect of siRNA $p<0.0001$, si*SCR* vs. si*PDGFRβ* $p<0.0001$, mock, siSCR, si*PDGFRβ* n=8 technical replicates, si*PDGFRα* n=5 technical replicates). Data are represented as means ± SEM. Numbers below Western blot panels represent relative quantification of the respective bands normalized to loading control by densitometry.

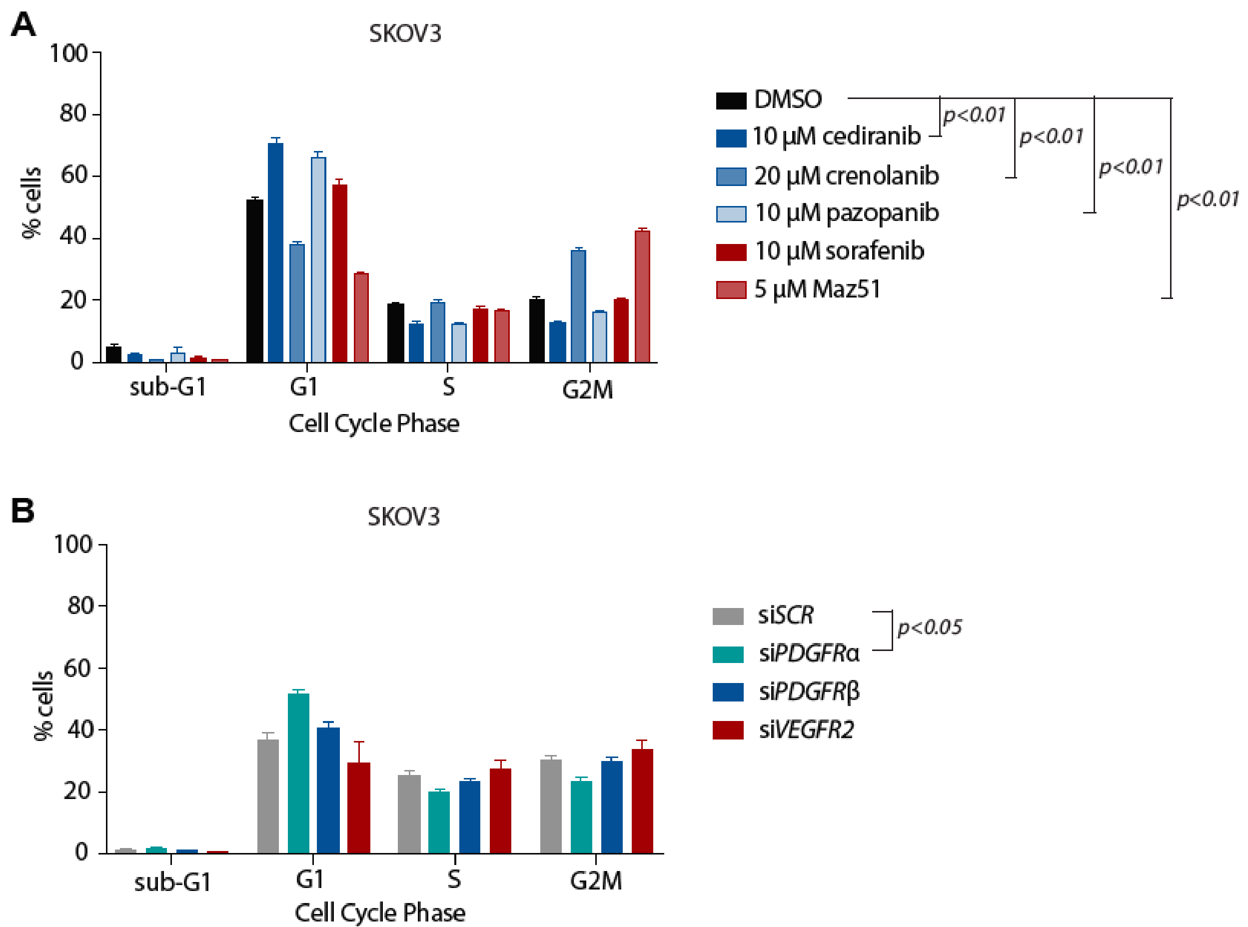

Fig. S6. No consistent changes were observed in cell cycle profiles after various kinase inhibitor and siRNA treatments. (A) Cell cycle profiles in SKOV3 cells 24 hours after treatment with small molecule kinase inhibitors (2-way ANOVA, interaction $p<0.001$, DMSO vs. 10 µM cediranib $p<0.01$, DMSO vs. 20 µM crenolanib $p=0.01$, DMSO vs. 10 µM pazopanib $p<0.01$, DMSO vs. 10 µM sorafenib $p=0.99$, DMSO vs. 5 µM Maz51 $p=0.001$; n=5-6 technical replicates). (B) Cell cycle profiles in SKOV3 cells 72 hours after treatment with siRNAs targeting *PDGFRα*, *PDGFRβ*, and *VEGFR2* (2-way ANOVA, interaction $p<0.001$, si*SCR* vs. si*PDGFRα* $p<0.05$, si*SCR* vs. si*PDGFRβ* $p=0.18$, si*SCR* vs. si*VEGFR2* $p=0.15$; n=5-6 technical replicates). Data are represented as means ± SEM.

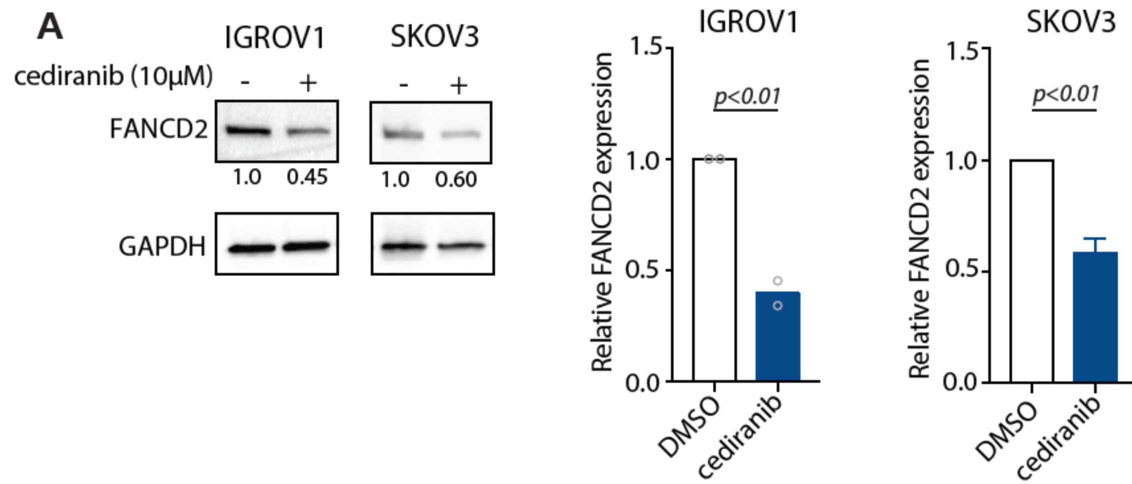

Fig. S7. Cediranib suppresses expression of FANCD2 in cancer cells in culture.
Western blot of FANCD2 expression in IGROV1 and SKOV3 cells treated with 10 µM cediranib in culture (unpaired t-test, IGROV1 $p<0.01$, SKOV3 $p<0.01$, n=2-3 technical replicates). Data are represented as means ± SEM. Numbers below Western blot panels represent relative quantification of the respective bands normalized to loading control by densitometry.

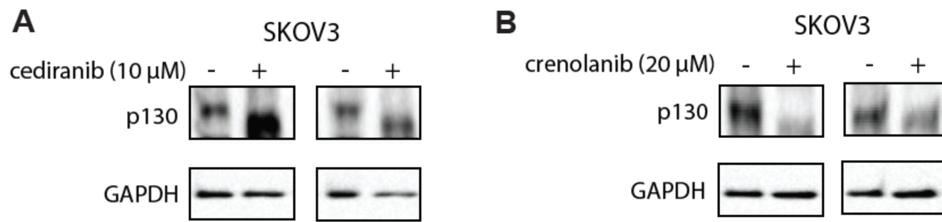

Fig. S8. PDGFR inhibition shifts migration of p130.
(A) Western blot of p130 in SKOV3 cells showing differential migration of p130 in SKOV3 cells after treatment with cediranib compared to controls (n=3 technical replicates). (B) Western blot of p130 in SKOV3 cells showing differential migration of p130 in SKOV3 cells after treatment with cediranib compared to controls (n=3 technical replicates).

Table S1. Reported mutations in DNA repair genes.
Cell Line Encyclopedia

Gene	IGROV1	SKOV3	MCF7	MDAMB231	U2OS	RKO
DNA Damage Recognition						
ATM	R248Q	X1413_splice				
ATR						
CHEK1	T226Hfs*14					
CHEK2						
Homology Directed Repair						
RBBP8	K357Nfs*3					
MRE11	R525K					
RAD50	K583Rfs*14					K583Rfs*14
NBN						
BRCA1	K654Sfs*47					D435Y
BRCA2	P3150T					N1784Tfs*7
RAD51						
RPA1						
EXO1						
PALB2	T787I					
BARD1						
RAD51B						S241P
RAD51C						
RAD51D						
XRCC3						
Non-Homologous End Joining						
PRKDC	I166Yfs*6					I166Yfs*6 L2891R
XRCC6						
XRCC5						
XRCC4						
LIG4						
NHEJ1						
DCLRE1C						
POLL						
POLM						
Fanconi Anemia Pathway						
FANCA						E345Vfs*63
FANCB						
FANCC						
FANCD2						
FANCE						S389P
FANCF						
FANCG						
FANCI						M807V
BRIP1						
FANCL						
SLX4						
ERCC4						

UBE2T							
FAAP100							
FAAP20							
FAAP24							
MUS81							
SLX1A							
XRCC2							

NCI-60

Gene	**IGROV1**	**SKOV3**	**MCF7**	**MDAMB231**
DNA Damage Recognition				
ATM	R248Q			
ATR				
CHEK1				
CHEK2				
Homology Directed Repair				
RBBP8				
MRE11	R525K			
RAD50				
NBN				
BRCA1				
BRCA2				
RAD51		X75_splice		
RPA1				
EXO1				
PALB2				
BARD1				
RAD51B				
RAD51C				
RAD51D				
XRCC3				
Non-Homologous End Joining				
PRKDC				
XRCC6				
XRCC5				
XRCC4			K197R	
LIG4				
NHEJ1				
DCLRE1C				
POLL				
POLM				
Fanconi Anemia Pathway				
FANCA				
FANCB				
FANCC				
FANCD2				
FANCE				
FANCF				

FANCG				
FANCI				
BRIP1				
FANCL				
SLX4				
ERCC4				
UBE2T				
FAAP100			L343P L348P C349S	
FAAP20				
FAAP24				
MUS81				
SLX1A				
XRCC2				